J|A|C|S
ARTICLES
Published on Web 07/29/2006

Site-Specific Nucleation and Growth Kinetics in Hierarchical Nanosyntheses of Branched ZnO Crystallites

Tierui Zhang, Wenjun Dong, Mary Keeter-Brewer, Sanjit Konar, Roland N. Njabon, and Z. Ryan Tian*

Contribution from the Department of Chemistry and Biochemistry, University of Arkansas, Fayetteville, Arkansas 72701

Received May 5, 2006; E-mail: rtian@uark.edu

Abstract: Here we report a site-specific sequential nucleation and growth route to the systematic building of hierarchical, complex, and oriented ZnO micro/nanostructures in solution nanosynthesis. Structures and morphologies of the products were confirmed by results from X-ray diffraction and scanning electron microscopy studies. The organic structure-directing agents (SDAs), diaminopropane and citrate, are found to play different roles in controlling the evolution of these new morphologies. Through the selective adsorptions of SDAs on different crystal facets of the primary ZnO rods, we have alternated the hierarchical growth of secondary and tertiary new complex nanostructures. Roles of the SDA concentration, nucleation time, and growth kinetics in the solution hierarchical ZnO nanosyntheses have all been systematically investigated.

Introduction

Zinc oxide (ZnO), a direct wide band gap (3.37 eV) semiconductor with a large excitation binding energy (60 meV), is one of the most important multifunctional oxide ceramic materials possessing a suite of useful properties[1,2] such as optical absorption and emission, piezoelectricity, transparent conductivity, high voltage−current nonlinearity, sensitivity to gases, and photocatalysis.[3] The interests in fabricating new ZnO nanostructures have been steadily growing due largely to the exciting new applications in (i) the room-temperature UV nanolasing[4] and (ii) the electricity generation from mechanical energy with high conversion efficiencies.[5]

Gas-phase[6−20] and solution-phase[21−35] syntheses are two main approaches adopted for the fabrication of ZnO nanostructures, each resulting in a long list of new morphologies reported in the literature. In the search for new methodologies and strategies to guide the design and solution syntheses of new morphologies, capping agents [e.g., ammonia, hydrazine, ethylenediamine, triethanolamine, tris(hydroxymethyl)aminomethane, dodecyl sulfate, citric acid, amino acids, peptides, gelatin, poly(vinyl alcohol), polyacrylamide, carboxyl-functionalized polyacrylamide, water-soluble diblock copolymers, etc.] have been successfully used to control sizes and shapes of ZnO nanocrystals.[36−50] However, the rich morphologies have also been found to be

(1) Look, D. C. *Mater. Sci. Eng. B* **2001**, *80*, 383.
(2) Fan, Z. Y.; Liu, J. G. *J. Nanosci. Nanotechnol.* **2005**, *5*, 1561.
(3) Maeda, K.; Takata, T.; Hara, M.; Saito, N.; Inoue, Y.; Kobayashi, H.; Domen, K. *J. Am. Chem. Soc.* **2005**, *127*, 8286.
(4) Huang, M. H.; Mao, S.; Feick, H.; Yan, H.; Wu, Y.; Kind, H.; Weber, E.; Russo, R.; Yang, P. *Science* **2001**, *292*, 1897.
(5) Wang, Z. L.; Song, J. H. *Science* **2006**, *312*, 242.
(6) Pan, Z. W.; Dai, Z. R.; Wang, Z. L. *Science* **2001**, *291*, 1947.
(7) Lao, J. Y.; Wen, J. G.; Ren, Z. F. *Nano Lett.* **2002**, *2*, 1287.
(8) Lao, J. Y.; Huang, J. Y.; Wang, D. Z.; Ren, Z. F. *Nano Lett.* **2003**, *3*, 235.
(9) Hu, J. Q.; Li, Q.; Meng, X. M.; Lee, C. S.; Lee, S. T. *Chem. Mater.* **2003**, *15*, 305.
(10) Hu, P.; Liu Y. Q.; Wang, X. B.; Fu, L.; Zhu, D. B. *Chem. Commun.* **2003**, *11*, 1304.
(11) Yan, H.; He, R.; Pham, J.; Yang, P. *Adv. Mater.* **2003**, *15*, 402.
(12) Yan, H.; He, R.; Johnson, J.; Law, M.; Saykally, R. J.; Yang, P. *J. Am. Chem. Soc.* **2003**, *125*, 4728.
(13) Wan, Q.; Yu, K.; Wang, T. H.; Lin, C. L. *Appl. Phys. Lett.* **2003**, *83*, 2253.
(14) Gao, P. X.; Wang, Z. L. *J. Am. Chem. Soc.* **2003**, *125*, 11299.
(15) Li, F.; Ding, Y.; Gao, P. X.; Xin, X. Q.; Wang, Z. L. *Angew. Chem., Int. Ed.* **2004**, *43*, 5238.
(16) Kong, X. Y.; Ding, Y.; Yang, R. S.; Wang, Z. L. *Science* **2004**, *303*, 1348.
(17) Gao, P. X.; Ding, Y.; Mai, W. J.; Hughes, W. L.; Lao, C. S.; Wang, Z. L. *Science* **2005**, *309*, 1700.
(18) Sun, X. H.; Lam, S.; Sham, T. K.; Heigl, F.; Jurgensen, A.; Wong, N. B. *J. Phys. Chem. B* **2005**, *109*, 3120.
(19) Shen, G. Z.; Bando, Y.; Liu, B. D.; Golberg, D.; Lee, C. J. *Adv. Funct. Mater.* **2006**, *16*, 410.
(20) Han, X. H.; Wang, G. Z.; Zhou, L.; Hou, J. G. *Chem. Commun.* **2006**, *2*, 212.
(21) Vayssieres, L.; Keis, K.; Hagfeldt, A.; Lindquist, S. E. *Chem. Mater.* **2001**, *13*, 4395.
(22) Guo, L.; Ji, Y. L.; Xu, H. B.; Simon, P.; Wu, Z. Y. *J. Am. Chem. Soc.* **2002**, *124*, 14864.
(23) Wang, Z.; Qian, X. F.; Yin, J.; Zhu, Z. K. *Langmuir* **2004**, *20*, 3441.
(24) Gao, X. P.; Zheng, Z. F.; Zhu, H. Y.; Pan, G. L.; Bao, J. L.; Wu, F.; Song, D. Y. *Chem. Commun.* **2004**, *12*, 1428.
(25) Li, Z. Q.; Ding, Y.; Xiong, Y. J.; Yang, Q.; Xie, Y. *Chem. Eur. J.* **2004**, *10*, 5823.
(26) Liu, B.; Yu, S. H.; Zhang, F.; Li, L. J.; Zhang, Q.; Ren, L.; Jiang, K. *J. Phys. Chem. B* **2004**, *108*, 4338.
(27) Liu, B.; Zeng, H. C. *J. Am. Chem. Soc.* **2004**, *126*, 16744.
(28) Kim, J. Y.; Osterloh, F. E. *J. Am. Chem. Soc.* **2005**, *127*, 10152.
(29) Mo, M.; Yu, J. C.; Zhang, L. Z.; Li, S. K. A. *Adv. Mater.* **2005**, *17*, 756.
(30) Umetsu, M.; Mizuta, M.; Tsumoto, K.; Ohara, S.; Takami, S.; Watanabe, H.; Kumagai, I.; Adschiri, T. *Adv. Mater.* **2005**, *17*, 2571.
(31) Yu, H. D.; Zhang, Z. P.; Han, M. Y.; Hao, X. T.; Zhu, F. R. *J. Am. Chem. Soc.* **2005**, *127*, 2378.
(32) Liang, J. B.; Liu, J. W.; Xie, Q.; Bai, S.; Yu, W. C.; Qian, Y. T. *J. Phys. Chem. B* **2005**, *109*, 9463.
(33) Munoz-Espi, R.; Qi. Y.; Lieberwirth, I.; Gomez, C. M.; Wegner, G. *Chem. Eur. J.* **2005**, *12*, 118.
(34) Hsu, J. W. P.; Tian, Z. R.; Simmons, N. C.; Matzke, C. M.; Voigt, J. A.; Liu, J. *Nano Lett.* **2005**, *5*, 83.
(35) Zhao, F. H.; Lin, W. J.; Wu, M. M.; Xu, N. S.; Yang, X. F.; Tian, Z. R.; Su, Q. *Inorg. Chem.* **2006**, *45*, 3256.
(36) Oner, M.; Norwig, J.; Meyer, W. H.; Wegner, G. *Chem. Mater.* **1998**, *313*, 115.
(37) Taubert, A.; Glasser, G.; Palms, D. *Langmuir* **2002**, *18*, 4488.
(38) Taubert, A.; Palms, D.; Weiss, O.; Piccini, M. T.; Batchelder, D. N. *Chem. Mater.* **2002**, *14*, 2594.
(39) Taubert, A.; Kubel, C.; Martin, D. C. *J. Phys. Chem. B* **2003**, *107*, 2660.

10.1021/ja0631596 CCC: $33.50

affected by experimental parameters such as the precursor type and concentration, type of solvent, solution pH, reaction temperature and time, template type, etc.[51−54] Along with the syntheses of semiconducting nanotetrapods,[55−59] systematic shape-controlled syntheses of hierarchical and branched complex ZnO nanostructures are emerging as new challenges in ZnO nanosyntheses.

Lately, roles of the sodium citrate and organoamines in hierarchical nanosyntheses of new ZnO morphologies have been studied separately.[60−62] However, these roles have not been systematically evaluated, and the related fundamental issues on how to control the site-specific nucleation pattern and growth kinetics have not been elucidated.

Hence, we have conducted a series of systematic synthesis studies in an attempt to reveal the kinetics and the roles of organic structure-directing agents (SDAs) (e.g., citrate, diaminopropane or DAP) in the formation of (i) secondary and tertiary ZnO nanobranches and (ii) nanoplates on the selected facets of these ZnO crystallites. To further prove the roles of the SDAs, we have also switched these two different SDAs in the ZnO solution nanosynthesis back and forth. In so doing, we have profoundly understood the roles of each SDA, and on that basis harvested a family of new ZnO branched structures with precisely controlled morphologies and spatial organization at the nanoscale. These systematic studies on the sequential evolution of the new nanostructures have enabled us to deduce the heterogeneous nucleation time and growth rate for the secondary branches on the primary rods. To our knowledge, these results are among the first obtained in hierarchical ZnO nanosynthesis. This work may provide us with a new rationale pertaining to the design and hierarchical solution synthesis of complex, ordered nanostructures of new types based on the needs in fundamental and application studies.

(40) Hoffmann, R. C.; Jia, S. J.; Bartolome, J. C.; Fuchs, T. M.; Bill, J.; Graat, P. C. J.; Aldinger, F. *J. Euro. Ceram. Soc.* **2003**, *23*, 2119.
(41) Liu, B.; Zeng, H. C. *Langmuir* **2004**, *20*, 4196.
(42) Zhang, H.; Yang, D. R.; Li, D. S.; Ma, X. Y.; Li, S. Z.; Que, D. L. *Cryst. Growth Des.* **2005**, *5*, 547.
(43) Li, P.; Wei, Y.; Liu, H.; Wang, X. K. *J. Solid State Chem.* **2005**, *178*, 855.
(44) Kuo, C. L.; Kuo, T. J.; Huang, M. H. *J. Phys. Chem. B* **2005**, *109*, 20115.
(45) Xu, L. F.; Guo, Y.; Liao, Q.; Zhang, J. P.; Xu, D. S. *J. Phys. Chem. B* **2005**, *109*, 13519.
(46) Konar, S.; Tian, Z. R. *J. Phys. Chem. B* **2006**, *110*, 4054.
(47) Gerstel, P.; Hoffmann, R. C.; Lipowsky, P.; Jeurgens, L. P. H.; Bill, J.; Aldinger, F. *Chem. Mater.* **2006**, *18*, 179.
(48) Bauermann, L. P.; Bill, J.; Aldinger, F. *J. Phys. Chem. B* **2006**, *110*, 5182.
(49) Bauermann, L. P.; del Campo, A.; Bill, J.; Aldinger, F. *Chem. Mater.* **2006**, *18*, 2016.
(50) Peng, Y.; Xu, A. W.; Deng, B.; Antonietti, M.; Colfen, H. *J. Phys. Chem. B* **2006**, *110*, 2988.
(51) Zhang, J.; Sun, L. D.; Yin, J. L.; Su, H. L.; Liao, C. S.; Yan, C. H. *Chem. Mater.* **2002**, *14*, 4172.
(52) Pal, U.; Santiago, P. *J. Phys. Chem. B* **2005**, *109*, 15317.
(53) Yang, M.; Pang, G. S.; Jiang, L. F.; Feng, S. H. *Nanotechnology* **2006**, *17*, 206.
(54) Zhou, X. F.; Chen, S. Y.; Zhang, D. Y.; Guo, X. F.; Ding, W. P.; Chen, Y. *Langmuir* **2006**, *22*, 1383.
(55) Jun, Y.; Jung, Y.; Cheon, J. *J. Am. Chem. Soc.* **2001**, *123*, 5150.
(56) Jun, Y.; Lee, S.-M.; Kang, N.-J.; Cheon, J. *J. Am. Chem. Soc.* **2002**, *124*, 615.
(57) Manna, L.; Milliron, D. J.; Meisel, A.; Scher, E. C.; Alivisatos, A. P. *Nat. Mater.* **2003**, *2*, 382.
(58) Milliron, D. J.; Hughes, S. M.; Cui, Y.; Manna, L.; Li, J.; Wang, L.-W.; Alivisatos, A. P. *Nature* **2004**, *430*, 190.
(59) Kuang, Q.; Jiang, Z. Y.; Xie, Z. X.; Lin, S. C.; Lin, Z. W.; Xie, S. Y.; Huang, R. B.; Zheng, L. S. *J. Am. Chem. Soc.* **2005**, *127*, 11777.
(60) Tian, Z. R.; Voigt, J. A.; Liu, J.; Mckenzie, B.; Mcdermott, M. J. *J. Am. Chem. Soc.* **2002**, *124*, 12954.
(61) Tian, Z. R.; Voigt, J. A.; Liu, J.; Mckenzie, B.; Mcdermott, M. J.; Rodriguez, M. A.; Konishi, H.; Xu, H. F. *Nat. Mater.* **2003**, *2*, 821.
(62) Sounart, T. L.; Liu, J.; Voigt, J. A.; Hau, J. W. P.; Spoerke, E. D.; Tian, Z. R.; Jiang, Y. B. *Adv. Funct. Mater.* **2006**, *16*, 335.

Experimental Section

1. Sample Preparations. All of the reagents (analytical grade purity) were purchased from Aldrich Chemical Co. They were all used directly without any further purification.

1.1. Synthesis of Sample I (Oriented Primary ZnO rods). First, a Teflon bottle was filled with 30 mL of the aqueous solution containing 20 mM of both $Zn(NO_3)_2$ and hexamethylenetetramine (HMT). To prepare primary ZnO rods standing up on glass, the glass substrates (microslide, VWR) were placed in the bottle that was then sealed and hydrothermally heated overnight at 60 °C (Figure 1a).

1.2. Synthesis of Sample II (Secondary Needlelike Nanobranches on the Primary ZnO Rods). After washing and drying in air, the sample I was incubated again at 60 °C for 6 h in an aqueous solution of 20 mM $Zn(NO_3)_2$ and HMT, together with the DAP (diaminopropane) ranging from 17.5 to 140.0 mM. Afterward, highly oriented arrays of secondary branched nanocrystals were grown on the columnar facets of primary ZnO rods with tunable sizes and spatial organizations (panels b−i of Figure 1).

1.3. Time Variations in Hierarchical Nanosyntheses. For the study of the effect of time on the morphological evolution, sample I was incubated at 60 °C from 0.5 to 24 h in an aqueous solution containing 20 mM of $Zn(NO_3)_2$ and HMT, and 87.5 mM DAP (Figure 2). The kinetics and nucleation time have been worked out from the plot of the branch length versus the time (Figure 3).

1.4. Synthesis of Sample III (Secondary Nanoplates on the Primary ZnO Rods). The procedure is similar to that for preparing sample II except that the DAP was replaced by sodium citrate (0.0566−0.226 mM). Oriented secondary nanoplates were formed on the columnar facets of the primary ZnO rods with controllable morphologies (Figure 4).

1.5. Synthesis of Sample IV (Tertiary Nanoplates on the Sample II Secondary Branches). Sample II from the secondary growth was incubated at 60 °C for 24 h in an aqueous solution of 20 mM $Zn(NO_3)_2$ and HMT, and 0.226 mM sodium citrate. Such an SDA switch in the tertiary growth has resulted in a new type of hierarchical and complex crystals labeled as sample IV (Figure 5).

1.6. Synthesis of Sample V (Tertiary Nanobranches on the Sample III Nanoplates). Sample III from the secondary growth was incubated at 60 °C for 6 h in an aqueous solution of 20 mM $Zn(NO_3)_2$ and HMT, and 87.5 mM DAP. After the hydrothermal treatment, a new kind of hierarchical and complex crystals was generated as a consequence of the SDA switch in the tertiary growth (Figure 6).

2. Sample Characterizations. The phase purity and spatial organization of ZnO micro/nanostructures were characterized by a Philips X'PERT X-ray diffractometer (45 kV, 40 mA, Cu Kα $\lambda = 1.5418$ Å with a graphite monochromator) scanning from 10° to 80° (2θ) at a speed of 1 °/min. The yields and morphologies of these crystalline structures were mainly investigated under a Philips ESEM XL30 scanning electron microscope equipped with a field emission gun and operated at 10 kV.

Results and Discussions

1. DAP-Induced Site-Specific Nucleation and Secondary Growth. Understanding the nucleation and growth kinetics in solution nanosynthesis is of significance in fundamental crystal science. The use of organic species for controlling the inorganic crystal growth has been extensively studied, especially in the recently reported solution syntheses of colloid nanocrystals.[63−69] However, the systematics that can reveal the stepwise profiles of the nucleation and growth have seldom been reported,[37−39] due probably to the fast kinetics taking place in the low nanoscale. Thus, we have purposely designed the above-mentioned six syntheses using relatively large ZnO crystallites to systematically study the site-specific nucleation, directional

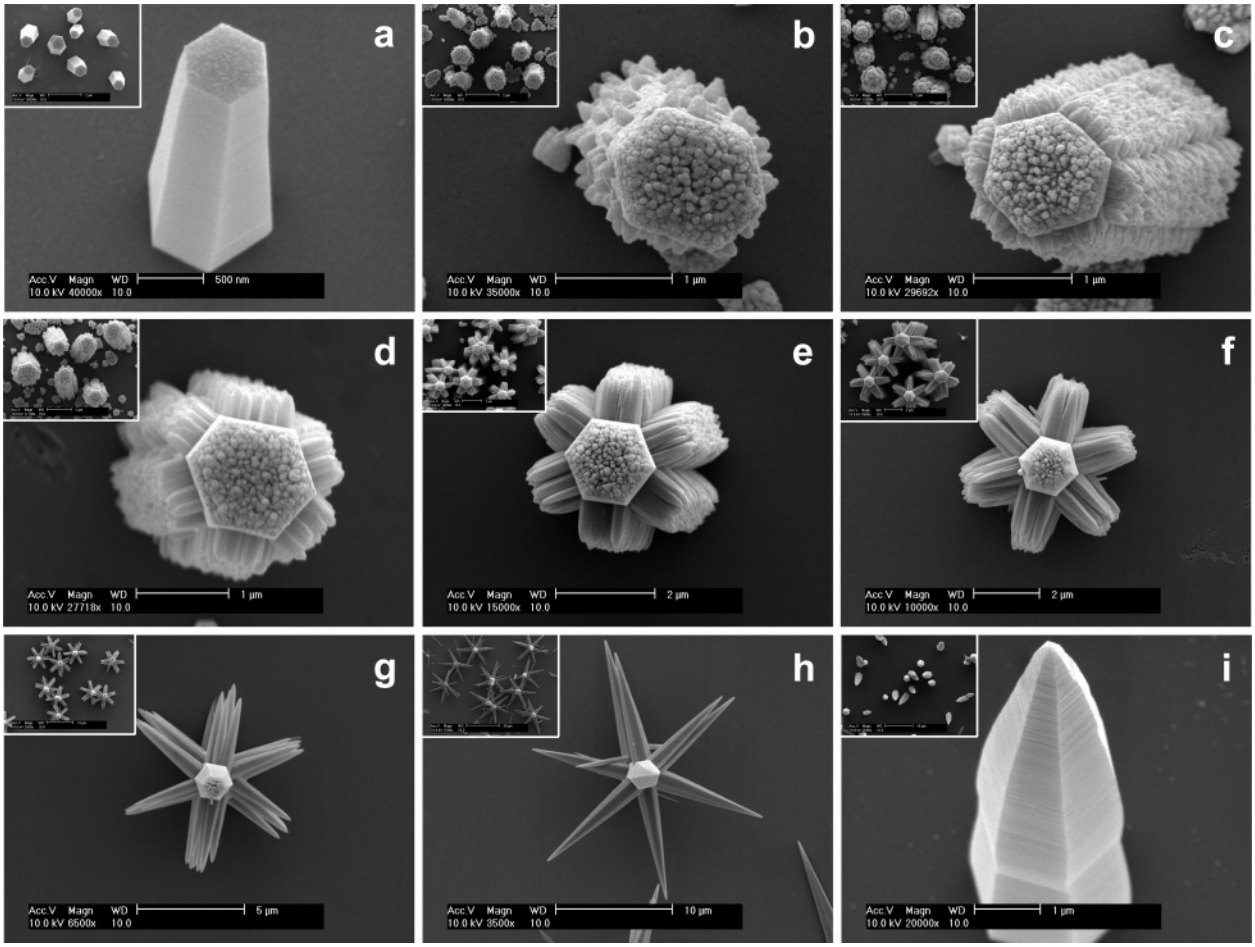

Figure 1. SEM photographs showing the systematics for the DAP concentration-dependent hierarchical growths. Highly oriented primary ZnO rods are shown in (a); (b−i) secondary needlelike crystalline branches formed by adding DAP 17.5 mM (b), 35.0 mM (c), 52.5 mM (d), 70.0 mM (e), 87.5 mM (f), 105.0 mM (g), 122.5 mM (h), and 140.0 mM (i). Each inset shows the corresponding low-magnification SEM survey photograph for that sample.

growth behavior, and kinetics in the solution hierarchical nanosynthesis.

Figure 1a shows the SEM photographs of the primary ZnO rods standing up on a clean glass substrate. It can be seen that these rods have well-defined hexagonal crystallographic planes, about 800 nm in diameter and 1.5 μm in height, with the ⟨001⟩ direction nearly perpendicularly to the substrate. During the secondary growth after DAP was introduced into the system, new crystals grew on the columnar facets of the primary rods.

If less DAP was used, sparse, tapered ZnO nanostructures randomly grew on the columnar facets of these primary rods (Figure 1b). As the DAP concentration was increased sequentially in the next sample, dense and organized taperlike ZnO nanostructures almost covered the entire columnar facets (Figure 1c). These short tapered nanostructures grew into long, needlelike structures as more DAP was added (Figure 1d). As the DAP concentration was further increased, these secondary branches became longer (from about 1 to 10 μm), thicker (from about 250 nm to 1.7 μm, measured from the end of the branches), and fewer on every columnar facet of the primary rod (panels e−h, Figure 1). Such a secondary nucleation and growth mechanism would further imply that crafting one nanostructure onto another as such may need not only to understand but also to manage the surface chemistries on the nanostructures.

In literature, the lattice match is believed to be able to influence the orientation of the ZnO nanorod arrays.[4,34,70] Probably as a result of the misfit of less than 10% between the (001) facet of ZnO and the substrate surface [such as the (110) facet of sapphire, the (001) facet of GaN, or the (111) facet of silver], *c*-oriented ZnO nanorods can be grown epitaxially on these substrates. In the case of amorphous substrate (e.g., glass), however, Zhang et al. hypothesized that a wetting layer of ZnO formed on the glass substrate, prior to the nanorod growth in chemical vapor, is critical to the oriented growth of the ZnO nanorods.[71] Recently, Yang's group has reported a generalized method for growing a ∼10 nm-thick, textured ZnO nanocrystals with all *c*-axes normal to substrate of nearly any type[72] and proposed

(63) Murry, C. B.; Norris, D. J.; Bawendi, M. G. *J. Am. Chem. Soc.* **1993**, *115*, 8706.
(64) Peng, X.; Wickham, J.; Alivisatos, A. P. *J. Am. Chem. Soc.* **1998**, *120*, 5343.
(65) Kim, Y.-H.; Jun, Y.-W.; Jun, B.-H.; Lee, S.-M.; Cheon, J. *J. Am. Chem. Soc.* **2002**, *124*, 13656.
(66) Chen, Y.; Kim, M.; Lian, G.; Johnson, M. B.; Peng, X. *J. Am. Chem. Soc.* **2005**, *127*, 13331.
(67) Yin, Y.; Alivisatos, A. P. *Nature* **2005**, *437*, 664.
(68) Shevchenko, E. V.; Talapin, D. V.; Kotov, N. A.; O'Brien, S.; Murray, C. B. *Nature* **2006**, *439*, 55.
(69) Kumar, S.; Nann, T. *Small* **2006**, *2*, 316.
(70) Yan, M.; Zhang, H. T.; Widjaja, E. J.; Chang, R. P. H. *J. Appl. Phys.* **2003**, *94*, 5240.
(71) Zhang, H. Z.; Sun, X. C.; Wang, R. M.; Yu, D. P. *J. Cryst. Growth* **2004**, *269*, 464.
(72) Greene, L. E.; Law, M.; Tan, D. H.; Montano, M.; Goldberger, J.; Somorjai, G.; Yang, P. *Nano Lett.* **2005**, *5*, 1231.

that the first several atomic layers of ZnO would convert to the ⟨001⟩ orientation via a minor structural transformation.

On the other hand, the self-assembled monolayers (SAMs) of organic molecules on various solid substrates have been widely used to direct inorganic crystal growth including ZnO.[73−80] A main role of the SAMs is to decrease the activation energy of nucleation of inorganic crystals. The size, shape, orientation, crystalline phase, distribution density on solid substrates of inorganic crystals can be controlled by adjusting the chain structure, the terminating functional group, the packing, and the conformation of the SAMs molecules.

Further, twinning as the driving force has also been adopted to try to explain the nearly vertical organization of one ZnO nanorod on the columnar facet of another, which was formed through a vapor-transport and condensation process.[81] Liu et al. also reported the twinning growth of ZnO rods with their *c*-axes nearly normal to the columnar facets of another ZnO rod.[62] Both studies, however, have shown high-resolution transmission electron microscopy images with little explanation on the solution interface chemistry.

Hence, one could picture the site-specific heterogeneous nucleation and the secondary growth in our system. First of all, the preferred adsorption of the DAP on the columnar surfaces of the primary rod would raise the nearby pH and guide the formation of the first a few layers of the precipitation near the adsorbed DAP on the columnar surface, thus initiating the site-specific heterogeneous nucleation process. Thereafter, the first few atomic layers of the site-specific precipitation would facilitate the nearly vertical growth of the secondary branches.

Our preliminary results in another study have shown that poorly oriented ZnO branches grew on the columnar facets of the primary rods only when the diamine with a short hydrocarbon chain was used. That is to say that the diamine chain length may play a critical role in the formation of *c*-oriented ZnO branches, implying that the diamine chelating effect and/or the SAM stability might play certain roles here. We also found that the diamine concentration (or the diamine coverage on the ZnO) would help organize the secondary rods, suggesting the population of the heterogeneous nuclei on the columnar surfaces might also determine the final organization of the secondary rods. In our system, as the concentration of DAP increases from 17.5 to 140.0 mM at room temperature, the corresponding pH also increases from 8.2 to 11.1. That is to say that more DAP molecules would produce more OH^- ions in the solution, which in turn promotes the formation of more ZnO growth units or a faster growth kinetics. To clearly picture what truly governs the site-specific secondary nucleation and directional growth as such, our detailed studies including interface spectroscopic analysis and computational simulation of the adsorption of SDA on ZnO surfaces are concurrently ongoing.

As Zeng et al.[82] proposed, the needlelike branches can fuse side-by-side into each other (Figure 1f). The new results obtained here, however, further imply that most secondary branches are likely rooted on many secondary nucleation sites on the columnar facets of the primary crystal.

As the concentration increased, the basal facets of both branches and primary ZnO rods gradually became sharper on top. Obviously, too much adsorption (or coverage) of DAP on the columnar facets of the primary rods may hinder the secondary nucleation and the subsequent growth along the columnar directions, thus, in turn, relatively promoting the growth along the ⟨001⟩ direction. As a result, the fast growing (001) facets should gradually disappear (Figure 1h), revealing that the growth on the primary rod facets is always accompanied by the secondary and tertiary growths. Therefore, the secondary branches on the columnar facets became fewer and fewer as the DAP concentration was increased, eventually leading to the formation of a morphology with no branches at the very high DAP concentration (Figure 1i).

It can be clearly seen from the Figure 1i that the tapered structure is composed of numerous nanoplates "stacked" along the ⟨001⟩ axis. The tapered morphology is commonly seen in many reports concerning the ZnO solution syntheses with different formation mechanisms.[41,45,83,84] Normally, a relatively rapid growth may result in the formation of edge dislocations which are responsible for the tapered morphology.[39,84] The large ZnO crystallite systematically evolved as such may reveal an important fact: the tapered morphology would not be formed by high Miller Index faces but by the multidecked and coaxial nanoplates of ZnO. This fact can well explain the formation of the morphological hierarchies discussed in later sections of this paper.

Sporadically distributed small ZnO nanoparticles were concurrently nucleated and grown on the glass substrates during the secondary growth (see the insets in panels b−f in Figure 1). As the DAP concentration increased, the number of the small particles gradually decreased and finally disappeared (Figure 1g) due probably to the Oswald ripening.[85] Further increase of the DAP concentration would start to raise the pH of the solution, which would make the small ZnO crystals dissolve in the rather basic solution.

In panels c−h of Figure 1, an inset of the low-magnification SEM photograph is included in each photograph to illustrate the control over each sample's structure orientation, yield, purity, morphological uniformity, and the size distribution. Overall, Figure 1 shows a systematic control over the secondary heterogeneous nucleation and hierarchical growth in a solution nanosynthesis with the help of an organic SDA. Our currently ongoing studies mentioned in the above are expected to help explain the roles of the DAP's selective adsorption in the solution hierarchical synthesis. The systematics learned here are critical to the following work on the switches of interface

(73) Kuther, J.; Nelles, G.; Seshadri, R.; Schaub, M.; Butt, H. J.; Tremel, W. *Chem. Eur. J.* **1998**, *4*, 1834.
(74) Aizenberg, J.; Black, A. J.; Whitesides, G. M. *Nature* **1999**, *398*, 495.
(75) Aizenberg, J.; Black, A. J.; Whitesides, G. M. *J. Am. Chem. Soc.* **1999**, *121*, 4500.
(76) Meldrum, F. C.; Flath, J.; Knoll, W. *Thin Solid Films* **1999**, *348*, 188.
(77) Kovtyukhova, N. I.; Buzaneva, E. V.; Waraksa, C. C.; Martin, B. R.; Mallouk, T. E. *Chem. Mater.* **2000**, *12*, 383.
(78) Bill, J.; Hoffmann, R. C.; Fuchs, T. M.; Aldinger, F. *Z. Metallkd.* **2002**, *93*, 478.
(79) Turgeman, R.; Gershevitz, O.; Palchik, O.; Deutsch, M.; Ocko, B. M.; Gedanken, A.; Sukenik, C. N. *Cryst. Growth Des.* **2004**, *4*, 169.
(80) Turgeman, R.; Gershevitz, O.; Deutsch, M.; Ocko, B. M.; Gedanken, A.; Sukenik, C. N. *Chem. Mater.* **2005**, *17*, 5048.
(81) Zhan, J. H.; Bando, Y.; Hu, J. Q.; Golberg, D.; Kurashima, K. *Small* **2006**, *2*, 62.
(82) Liu, B.; Zeng, H. C. *J. Am. Chem. Soc.* **2003**, *125*, 4430.
(83) Hu, P. A.; Liu, Y. Q.; Fu, L.; Wang, X. B.; Zhu, D. B. *Appl. Phys. A* **2005**, *80*, 35.
(84) Tong, Y. H.; Liu, Y. C.; Shao, C. L.; Mu, R. X. *Appl. Phys. Lett.* **2006**, *88*, 123111.
(85) Horn, Q. C.; Shao-Horn, Y. *J. Electrochem. Soc.* **2003**, *150*, A652.

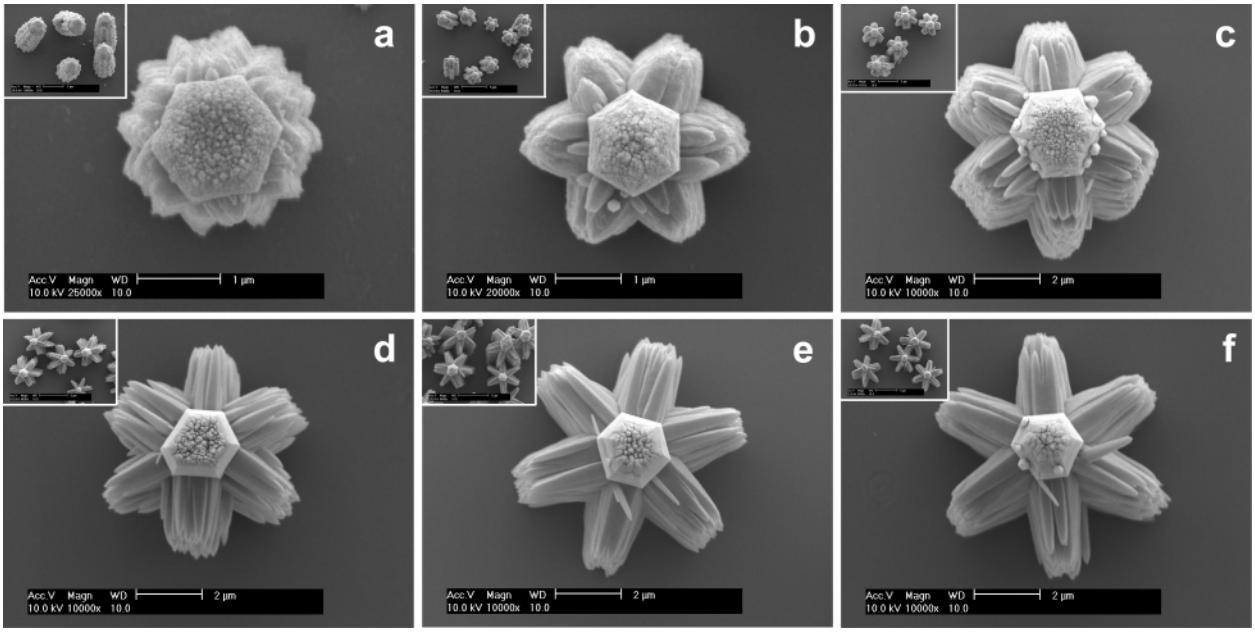

Figure 2. SEM photographs showing the time-dependent microprofile of the secondary growth in the system of 87.5 mM DAP. (a) 0.5 h; (b) 1.0 h; (c) 2.0 h; (d) 4 h; (e) 6 h; (f) 24 h. Each inset shows the corresponding low-magnification SEM survey photograph for that sample.

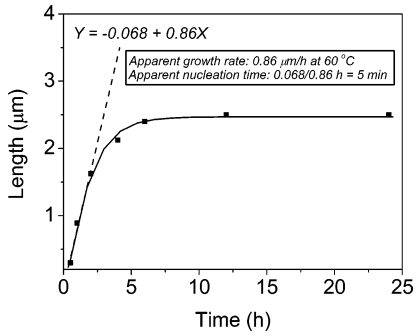

Figure 3. Plot of the average length of ZnO branches as a function of growth time, and the related kinetics.

chemistry not only to control the kinetics but also to alternate the morphologies in the ZnO hierarchical nanosynthesis purely by design.

2. Time Effect and Kinetics. To determine the growth kinetics in ZnO nanosynthesis, a tedious, time-dependent synthetic study was conducted in the reaction system with 87.5 mM DAP (Figure 2) at 60 °C. After the hydrothermal reaction for 0.5 h (Figure 2a), dense, tapered nanostructures about 275 nm in length grew on the columnar facets of the primary rods. After 2 h, the length of these branches reached about 1.7 μm (Figure 2c). From 2 to 6 h, the growth gradually became slower. After 6 h, the length of branches was about 2.4 μm, and the growth almost stopped (Figure 2, d and e). A longer reaction time (e.g., 24 h) does not elicit further growth of the branches (Figure 2f). As discussed above, the primary ZnO rods gradually grew into the tapered structures during the growth of the secondary branched crystallites.

Figure 3 shows that the growth of branches, depicted in Figure 2, is fast in the first 2 h, forming a linear correlation between the branch length and the reaction time ($Y = -0.068 + 0.86X$). The slope, 0.86 μm/h, represents an apparent growth rate for the branch growth along the ⟨001⟩ orientation within the first 2 h at 60 °C. Another important datum, the apparent nucleation time of 5 min, could also be obtained from this equation by extrapolating to the length to zero. This set of kinetic data would be among the first reported in hierarchical ZnO nanosynthesis, implying that some exciting fundamental science would be involved in the first few minutes in ZnO solution nanosynthesis.

Taubert et al. reported a detailed work on the kinetics and growth mechanism of ZnO particles in aqueous solutions containing two polymers, P(EO-*b*-MAA) and P(EO-*b*-SSH).[37,38] Different from these two polymers, DAP behaves not only as the SDA but also as the OH^- supplier, which was discussed in the above. Our preliminary results from another detailed study suggest that a higher DAP concentration results in a faster growth rate and shorter nucleation time of the secondary ZnO branches at a fixed temperature. Also in that study we observed that a higher temperature (>45 °C) would result in a faster growth rate and a shorter nucleation time. These two preliminary results have encouraged us to design and conduct the above-mentioned spectroscopic and simulation studies.

3. Revisit to the Citrate Effect. It has been reported in the literature[61] that citrate anions would preferably bind on the (001) facet of ZnO to prohibit the nucleation and crystal growth along the ⟨001⟩ orientation, thus providing a simple approach to controlling to the aspect ratio of the ZnO rods. As a synthetic revisit, we have systematically studied the citrate-induced secondary nucleation and growth of highly oriented ZnO primary rods on the substrate. Similarly, crystalline ZnO nanoplates grew on the columnar facets of the primary ZnO rods when citrate was introduced in the reaction system (Figure 4). When a small amount of citrate was added, sparse ZnO nanoplates with thickness from about 250 to 320 nm formed on the columnar facets of the primary ZnO rods. As the concentration of citrate increased further, the nanoplates became denser and thinner (Figure 4d), which is in a good agreement with the literature results.

4. Switching from DAP to Citrate in Sequential Hierarchical Nanosynthesis. The above systematic synthetic studies on two functionally different SDAs have provided us with a new synthetic method for design and development of new

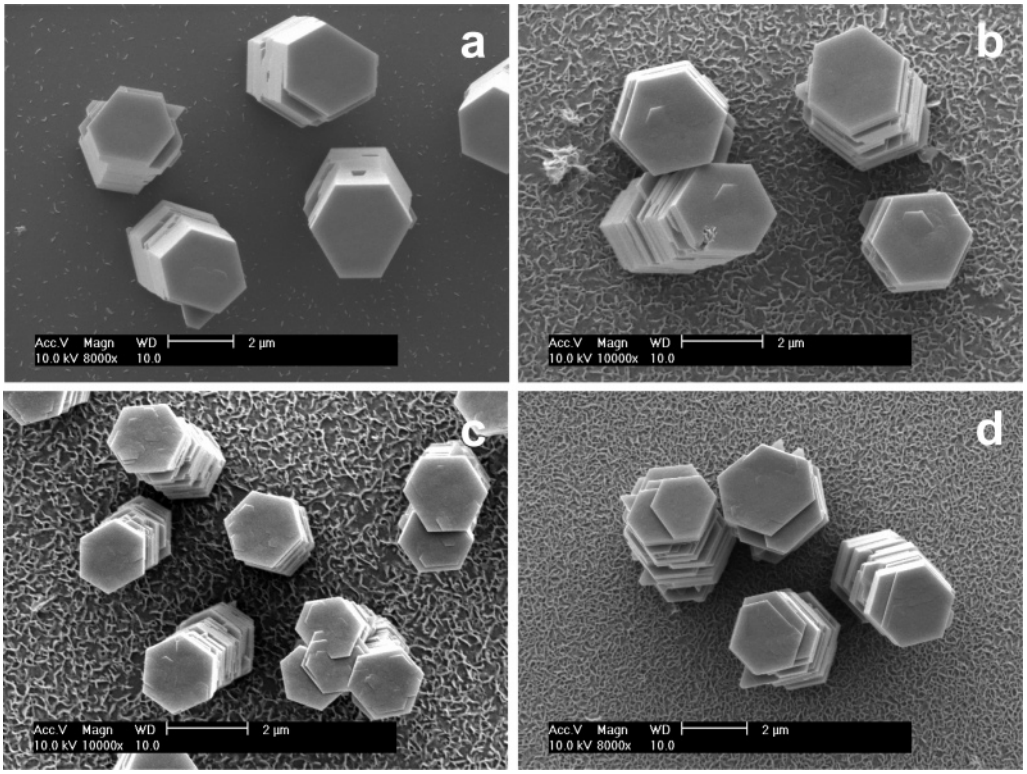

Figure 4. SEM photographs showing systematics for the citrate-induced hierarchical growths of secondary nanoplates on the primary rods. The citrate concentration used in each sample is (a) 0.0566 mM, (b) 0.113 mM, (c) 0.170 mM, (d) 0.226 mM.

solution routes in solid-state nanosynthesis. By rationally combining and alternating the uses of the DAP and citrate, new families of oriented and ordered complex crystallites in both nanometer and micrometer scales could be hierarchically synthesized from solutions.

The first design for the sequential hierarchical nanosyntheses is illustrated in Figure 5a. The sequence consists of the first growth of the oriented primary ZnO rods, the secondary growth of the branches on the columnar facets of primary rods using DAP, and the tertiary growth of the nanoplates on the columnar facets of both the primary rods and the secondary branches. XRD patterns in Figure 5b confirm the formation of each of these morphologies across the entire substrate. All of the XRD patterns can be indexed to the Wurtzite (hexagonal phase, space group $P6_3mc$) ZnO structure with calculated lattice constants $a = 3.252$ Å, $c = 5.210$ Å (JCPDS79-2205), which suggests that no other crystalline phases coexist in the samples.

The texture effect of the anisotropic morphology and orientation on the relative intensities of the diffraction peaks can be seen from these XRD data. For randomly oriented ZnO powders, (101) should be the dominant diffraction peak.[34] Here, only (002) and (004) peaks can be observed from sample I, indicating a highly uniform orientation of the primary rods on the substrate. The XRD pattern of sample II starts to show (100) and (101) diffraction peaks that are contributed by the secondary ZnO nanobranches each with the *c*-axis nearly parallel to the substrate surface. After the tertiary growth, ZnO nanoplates covered the columnar facets of both the secondary branches and the primary rods (Sample IV). Thus, sample IV has less (100) and (101) surfaces exposed to the incident X-ray in comparison to sample II, leading to a slight decrease in the relative intensities of (100) and (101) with respect to that of the (001) peak. The XRD data suggest that the samples on the substrate are pure in structure, morphology, and spatial organization, which is in line with the design shown in Figure 5a.

Figure 5c shows SEM photographs of highly oriented primary ZnO rods. The inset in Figure 5c from a low-magnification SEM survey shows the purity and yield of this synthesis, which is consistent with the XRD pattern (sample I in Figure 5b). Next, needlelike nanobranches were formed in the secondary growth due to the DAP (87.5 mM) effect (Figure 5d), also agreeing well with the XRD pattern (sample II in Figure 5b). After the tertiary growth, nanoplates were formed due to the citrate (0.226 mM) effect (Figure 5, e and f). The inset in Figure 5e shows both the purity and yield of this synthetic step, which agrees well with the XRD pattern (sample IV in Figure 5b).

The big branches (Figure 5, e and f) closely stack as such to have one in each layer on every columnar facet of the primary ZnO rods, which is likely resulted from the healing of the small secondary branches (Figure 5d). ZnO nanoplates with thicknesses from 100 to 250 nm covered the columnar facets of the primary rods and secondary branches. The stacked tertiary nanoplates are about 15−25 nm in thickness (Figure 5, e and f).

This would be among the first use of the rational design of sequential synthetic routes for hierarchically growing new solid-state complexes.[61] The precise control over the morphology and spatial organization in both nanometer and micrometer scales has been realized by switching the use of two different SDAs. Knowledge accumulated here has encouraged us to reverse the order of using the two different SDAs in a new sequential synthesis to further understand the roles of the two SDAs in ZnO nanosyntheses.

5. Switching from Citrate to DAP in Sequential Hierarchical Nanosynthesis. A new, sequential synthesis that resulted from switching the order for the secondary and tertiary growths in Figure 5 is schematically depicted in Figure 6a. The XRD

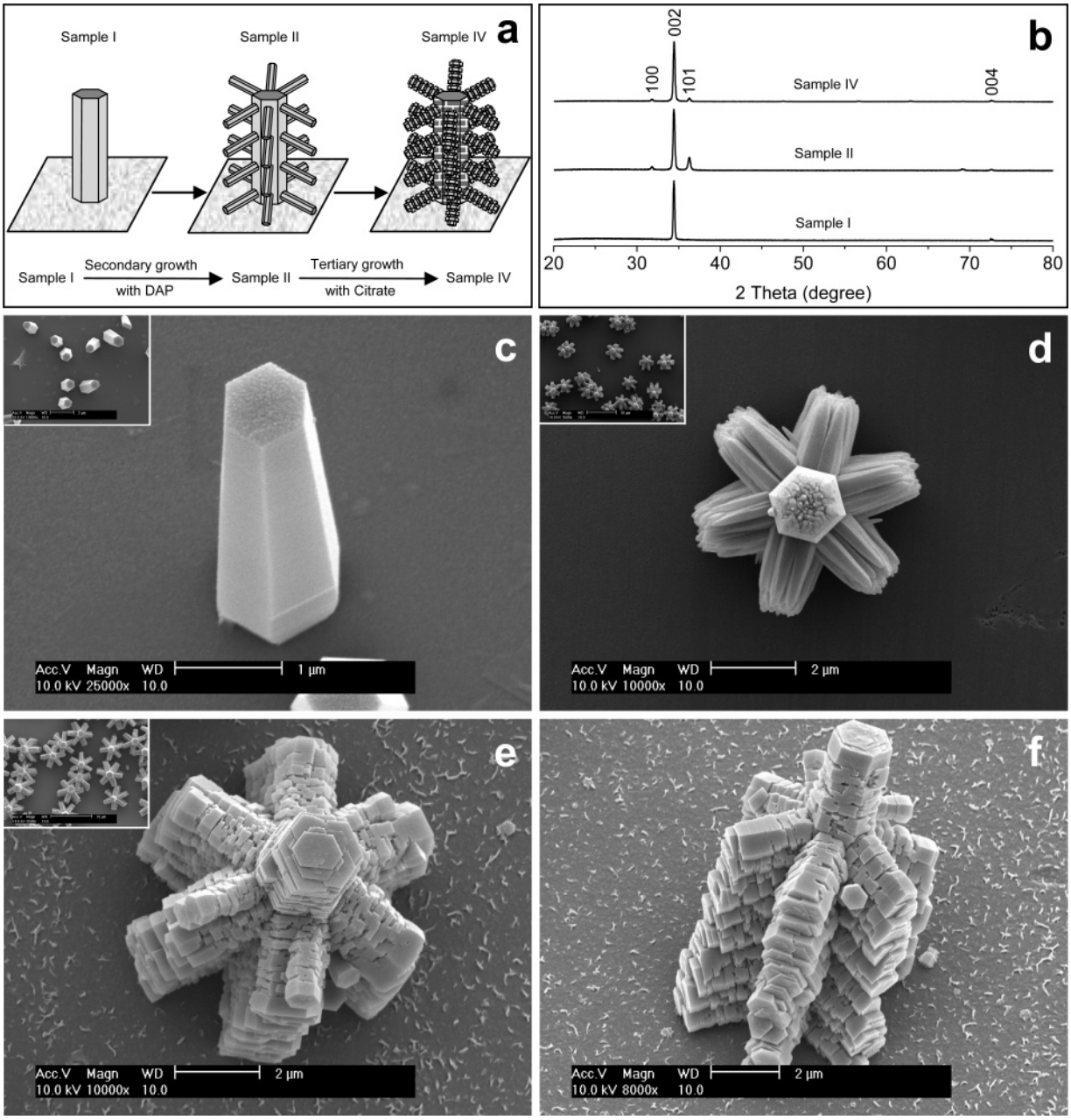

Figure 5. Morphological evolution of sample IV monitored by XRD and SEM: (a) Schematic illustration of the formation of sample IV; (b) XRD patterns of samples I, II, and IV; (c) SEM photos of sample I; (d) SEM photos of sample II; (e) SEM photo (top view) of sample IV; (f) SEM photo (side view) of sample IV. Each inset shows the corresponding low magnification SEM survey photograph for that sample.

pattern of sample III (see in Figure 6b) is similar to that of sample I due to the epitaxial growth of these ZnO nanoplates along the columnar facets of oriented primary rods, indicating an excellent orientation in the *c*-axis direction ⟨001⟩ for the oriented rods over a large area. After the tertiary growth, branches can grow from both edges of platelets and gaps between the plates, giving rise to the (100) and (101) diffraction peaks (see sample V, Figure 6b). Similarly, the high yield and purity observed here are the characteristics of the well-controlled sequential hierarchical synthesis, and the XRD data are as expected in Figure 6a.

The SEM photographs of samples I and III are respectively shown in c and d of Figure 6 , each agreeing well with its XRD pattern in Figure 6b. In sample V, needlelike tertiary branches about 2.4 μm in length were aligned (Figure 6e), intercrossing each other from different layers (Figure 6, e and f) of the secondary nanoplates and forming three groups on each columnar facet of the primary rods. In each of the three groups, tertiary branches at the secondary nanoplate edge are seen to bend outwardly. This grouped morphology is different from the parallel array of branches observed in Figure 5d.

Likely, the two edges of each nanoplate would be very reactive and, therefore, ideal for the tertiary nucleation and then the growth of the branches in a slanted manner along the upper and lower edges of the nanoplates, as illustrated in Figure 6a. In parallel, some rods grew nearly vertically from the gaps between any two adjacent secondary nanoplates (also see the depiction in Figure 6a) via the abovementioned heterogeneous nucleation and growth processes. It is believed that the morphology and spatial organization of secondary nanoplates (Figure 6d) have played an unusual structure-organizing role in the tertiary nucleation and crystal growth.

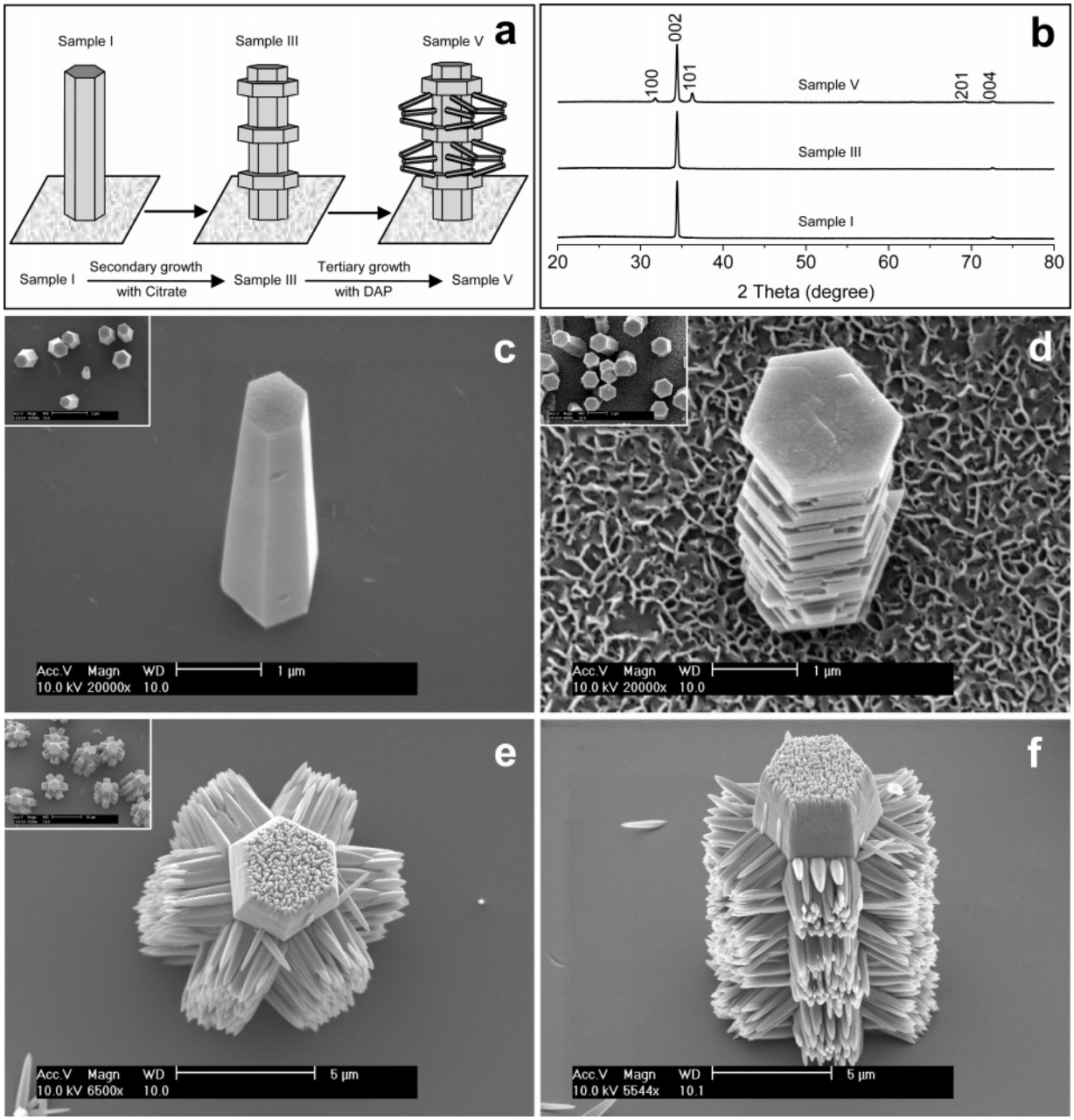

Figure 6. Morphological evolution of sample V monitored by XRD and SEM: (a) schematic illustration of the formation of sample V; (b) XRD patterns of samples I, III, and V; (c) SEM photos of sample I; (d) SEM photos of sample III; (e) SEM photo (top view) of sample V; (f) SEM photo (side view) of sample V. Each inset shows the corresponding low magnification SEM survey photograph for that sample.

Such a switch in the use of two different SDAs has resulted in a set of new hierarchical crystalline structures never reported before. The consistent and systematic data in Figures 5 and 6 have ultimately confirmed the role of each SDA in hierarchical nanosynthesis and encouraged us to perform detailed studies on surface analysis in combination with simulation and modeling studies.

Concluding Remarks

In this contribution, we have developed a mild, aqueous solution-systhesis approach to hierarchical growth of complex and oriented ZnO nanostructures by taking advantage of the preferential adsorption of SDAs on different facets of hexagonal ZnO crystals. The size, shape, and orientation of both secondary and tertiary structures can be controlled systematically. By alternating the use of different SDAs, new hierarchical and complex crystals were created as an exciting addition to the family of ZnO nanostructures.

These new, branched nanostructures may have unique application potential in the development of photonic, electronic, and sensing nanodevices. ZnO nanowires with branched structures have been used for constructing dye-sensitized solar cells with the energy conversion efficiency of 0.5% and internal quantum efficiency of 70%.[86] Dendritic nanowire ultraviolet laser arrays have been developed using the ZnO comblike nanostructures.[12] Flowerlike ZnO nanostructures have been employed for making ethanol sensors with low resistance and high sensitivity.[87] In addition, the photocatalytic efficiency of

(86) Baxter, J. B.; Aydil, E. S. *Appl. Phys. Lett.* **2005**, *86*, 053114.

oriented ZnO nanoplates is nearly twice that of oriented ZnO rods.[61] Therefore, we expect that our new branched/plated ZnO nanostructures may help advance the above-mentioned nanotechnologies.

Thus, this work sheds new light on rational design and truly hierarchical syntheses of application-targeted functional materials from nanometer to micrometer scales. In addition, this contribution enhances our understanding of the fundamental science that governs the interfacial chemistry between two differently structured nanoscale building blocks.

Acknowledgment. The project has been supported by a start-up grant from the University of Arkansas and a grant from the ABI. T.Z. thanks A. Tolland and J. Shultz of Arkansas Analytical Lab (AAL) for their help with the FESEM and XRD studies.

JA0631596

(87) Feng, P.; Wan, Q.; Wang, T. H. *Appl. Phys. Lett.* **2005**, *87*, 213111.